

## Gamma-ray linear polarization measurements following heavy-ion bombardment of odd isotopes of Pd<sup>†</sup>

Jin Soon Kim and Y. K. Lee

*The Johns Hopkins University, Baltimore, Maryland 21218*

K. A. Hardy

*Florida International University, Miami, Florida 33144*

P. C. Simms, J. A. Grau, G. J. Smith,\* and F. A. Rickey

*Purdue University, Lafayette, Indiana 47907*

(Received 24 February 1975)

$\gamma$ -ray linear polarization measurements have been used to locate negative parity states in the even-odd isotopes  $^{99,101,103}\text{Pd}$ . A Compton polarimeter based on two Ge(Li) coaxial detectors was used. Collective bands ( $I = \frac{11}{2}^-, \frac{15}{2}^-, \frac{19}{2}^-, \dots$ ) built on  $\frac{11}{2}^-$  states were observed in  $^{101}\text{Pd}$  and  $^{103}\text{Pd}$ . Many negative parity states were also observed in  $^{99}\text{Pd}$ , but they do not appear to be part of a similar collective band. These polarization measurements also confirm many angular momentum assignments which previously had been made using systematic arguments.

[ NUCLEAR REACTIONS  $^{90,92,94}\text{Zr}(^{12}\text{C}, 3n)$ ,  $E = 48\text{--}56$  MeV; measured linear polarization of  $\gamma$  rays; parities and multipole mixing ratios in  $^{99,101,103}\text{Pd}$  transitions deduced. ]

### I. INTRODUCTION

In recent experiments<sup>1</sup> unusual collective structure has been found in the odd- $A$  nuclei  $^{101,103,105}\text{Pd}$ . Cascades of  $\gamma$  rays have been observed coming from states which are apparently members of quasisrotational bands. The bandheads are relatively pure single-quasiparticle states. The linear polarization measurements described here are part of a systematic study of these unusual collective bands.

The parity of states in a band can be established by determining the change in parity associated with the decay of the bandhead.  $\gamma$ -ray linear polarization measurements provide a direct way to determine this change in parity. Linear polarization measurements are also very useful for determining mixing ratios and for removing ambiguities in spin assignments which have been made from  $\gamma$ -ray angular distributions.

Systematic trends suggest that there should be a relatively low lying  $\frac{11}{2}^-$  state in  $^{101}\text{Pd}$  and  $^{103}\text{Pd}$  (essentially due to an  $h_{11/2}$  quasiparticle). This state was previously known<sup>2</sup> in  $^{105}\text{Pd}$  and is the bandhead for one of the quasisrotational bands. Thus a primary aim of these experiments was to locate the  $\frac{11}{2}^-$  states in  $^{101}\text{Pd}$  and  $^{103}\text{Pd}$ . The linear polarization measurements confirm the expectation that the  $\frac{11}{2}^-$  state serves as a bandhead in both  $^{101}\text{Pd}$  and  $^{103}\text{Pd}$ . However the results in  $^{99}\text{Pd}$  are quite different. A series of negative

parity states was observed, but they are apparently not due to a quasisrotational band.

### II. EXPERIMENTAL PROCEDURES

The heavy ions were accelerated in the Purdue FN tandem Van de Graaff accelerator. The odd isotopes  $^{99,101,103}\text{Pd}$  were obtained by the ( $^{12}\text{C}, 3n$ ) reaction using enriched targets of  $^{90,92,94}\text{Zr}$ , respectively. The beam energy was 48 MeV for the  $^{92,94}\text{Zr}$  targets and 56 MeV for the  $^{90}\text{Zr}$  target.

The decay scheme and deexcitation  $\gamma$  rays were previously identified by  $\gamma$ - $\gamma$  coincidence work and excitation function experiment. After the major features of the decay scheme were established, all the spectra were reexamined for weak  $\gamma$  rays—particularly for those emitted in crossing transitions between bands. The angular distributions of  $\gamma$  rays were also previously measured.

In the present experiment we use the scheme discussed by Taras<sup>3</sup> and by Hardy *et al.*<sup>4</sup> in which the linear polarization of deexcitation  $\gamma$  rays is measured only at one angle with respect to the beam direction. A separate measurement of angular distribution of the  $\gamma$  rays under the identical experimental conditions is carried out in order to provide the angular distribution parameters.

The principle of construction of a polarimeter by symmetric arrangement of two Ge(Li) crystals around the axis of rotation has been described previously<sup>4,5</sup> and its application to high spin states

reached by (HI,  $xn$ ) reaction has been discussed.<sup>5</sup> The only important feature of the present polarimeter not discussed in the above papers is the fact that two true-coaxial Ge(Li) detectors are now mounted in the same cryostat, and the whole cryostat is rotated instead of the crystals alone (see Fig. 1).

The polarimeter was designed with high counting efficiency in mind for application to heavy-ion reactions using a tandem accelerator. Two crystals are almost side by side in order to increase the coincidence rate, and each crystal is used as a scatterer and a counter of the Compton-scattered  $\gamma$  ray simultaneously. One may call this a diffuse geometry achieving only one-half of the possible asymmetry ratio with ideal geometry. However, the present arrangement is the outcome of consideration of various experimental results including typical yields of the (HI,  $xn$ ) reaction, the need to take data rapidly because of the typi-

cal scheduling problems of accelerators, and the maximum single counting rate permissible in each crystal without deterioration of energy resolution. Since the asymmetry ratio is energy dependent, and the effective size of the scatterer as well as counter is also energy dependent, one cannot optimize the size of the detector for general purposes. The present arrangement is such that when the polarimeter is located at a sufficient distance from the target to avoid solid angle corrections, each crystal counts roughly 10 000  $\gamma$  rays per second with an average carbon or oxygen beam readily available for (HI,  $xn$ ) reactions.

In the present apparatus each cylindrical Ge(Li) detector was 40 mm in diameter and 21 mm in height. The detector had a cylindrical dead region of 7 mm in diameter at the center. The two detectors were mechanically cut to the same size and matched closely to each other in resolution and efficiency. The detectors are so-called "true-coaxial" detectors in which cylindrical symmetry is emphasized and the uniform radial electric field is maintained in order to achieve uniform and fast rise of pulses for timing.

The energy resolution of the sum spectra was 5 keV for a  $\gamma$  ray of 1 MeV, compared to the 3 keV resolution of a single detector. The degradation of resolution in the sum was mainly due to the nonlinearity in the two channels. This observation was confirmed in a later experiment where the pulse height information were accumulated in a two parameter mode and summed later in a computer after correction of the nonlinearity.

### III. ANALYSIS

The linear polarization  $P$  can be defined as:

$$P = \frac{I(0^\circ) - I(90^\circ)}{I(0^\circ) + I(90^\circ)},$$

where  $I(0^\circ)$  and  $I(90^\circ)$  are the intensities of the  $\gamma$  rays which have their  $E$  vector parallel and perpendicular to the reaction plane, respectively. For a pure multipole transition  $P$  is determined solely by the angular distribution coefficients ( $A_{22}$  and  $A_{44}$ ) and the parity change:

$$P = \pm \frac{3A_{22}H_2(\delta) + 1.25A_{44}H_4(\delta)}{2 - A_{22} + 0.75A_{44}} \begin{array}{l} + \text{no parity change} \\ - \text{parity change} \end{array}$$

where  $H_k(\delta) = 1$  if the transition is pure ( $\delta = 0$  or  $\infty$ ). When  $A_{22}$  and  $A_{44}$  are known from angular distribution measurements which are made with essentially the same experimental conditions, the sign of  $P$  is sufficient to determine the parity change of a pure transition.

The linear polarization provides no information about angular momentum changes for pure transi-

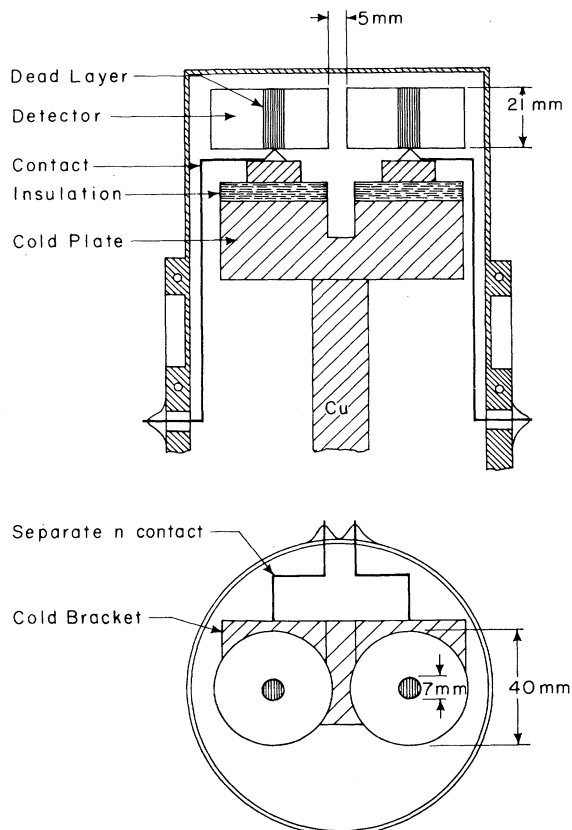


FIG. 1. Schematic diagram of the Compton polarimeter based on two true coaxial Ge(Li) detectors. The polarimeter was mounted on a vertical dip stick partially shown here. The whole assembly of the vacuum jacket and the dip stick were rotated around a vertical axis by remote control.

tions, but it can be very useful for mixed transitions.  $H_k(\delta)$  is given by the following formula for a dipole-quadrupole mixture ( $L=1$  and  $L'=2$ ):

$$H_2(\delta) = \frac{F_2(LL) - \frac{2}{3}\delta F_2(L, L') + \delta^2 F_2(L', L')}{F_2(LL) + 2\delta F_2(L, L') + \delta^2 F_2(L', L')}$$

$$H_4(\delta) = 1.$$

The  $F_k$  functions are standard (e.g., see Ref. 6). The sign convention of Krane and Steffen<sup>7</sup> is used in defining the mixing ratio  $\delta$ .

$$\delta = \langle I_i | L' | I_f \rangle / \langle I_i | L | I_f \rangle.$$

The linear polarization  $P$  was measured by observing the relative difference between the counting rates  $N(0^\circ)$  and  $N(90^\circ)$  obtained with the plane containing the detector axis oriented parallel and perpendicular to the reaction plane, respectively. Since the Compton scattering is most probable in a direction perpendicular to the  $E$  vector,  $N(90^\circ)$  will be greater than  $N(0^\circ)$  when  $P$  is positive.

Thus  $\Delta$  is defined as

$$\Delta = \frac{N(90^\circ) - N(0^\circ)}{N(90^\circ) + N(0^\circ)}$$

so that the polarization efficiency of the analyzer is a positive number defined by the expression

$$Q = \Delta/P.$$

The efficiency  $Q$  is a characteristic number of the particular instrument, but it is dependent to some extent on the setting of the discrimination level of energy signals accepted for analysis.<sup>4</sup> However, such dependence on discrimination level is small when the  $\gamma$  ray energy is above 250 keV which is the case for the present experiment. The instrument is calibrated with  $\gamma$  rays ranging in energy from 261 to 1700 keV from the nuclei of <sup>41</sup>K, <sup>101</sup>Pd, and <sup>24</sup>Mg. The calibration points shown in Fig. 2 are all produced by  $E2$  transitions except for the lowest energy point which is the 261 keV pure  $M1$  transition<sup>8</sup> in <sup>101</sup>Pd. The solid curve was obtained by the least squares fit of the data from the four nuclei to a curve

$$Q = Q_0(a + bx)$$

in which  $Q_0$  is the efficiency for the ideal case of two point detectors. In our arrangement  $Q_0$  can easily be shown by Klein-Nishina formula to be,

$$Q_0 = \frac{1 + \alpha}{1 + \alpha + \alpha^2},$$

where

$$\alpha = h\nu/m_0c^2.$$

The geometrical diffuseness in our practical arrangement will reduce the value  $Q$  from the ideal

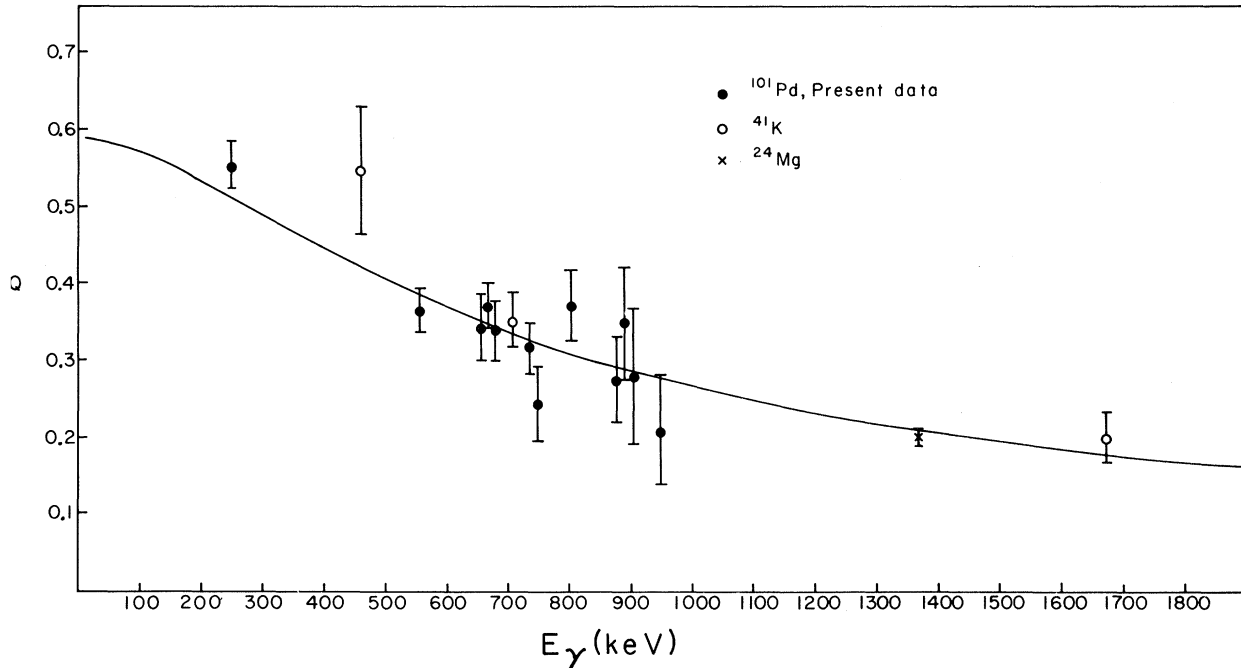


FIG. 2. The asymmetry ratio as a function of the incident  $\gamma$ -ray energy. The curve is the least squares fit to the experimental points assuming a shape derived from the ideal geometry multiplied by a shape correction factor which was linear in energy.

case of  $Q_0$ , but the shape of the curve will not change much since the curve  $Q_0$  is a slowly varying function. Therefore, the calibration curve is envisaged to have the same shape as  $Q_0$  with a correction factor which is linear in energy. The least squares fit gives

$$a = 0.5848 ,$$

$$b = 0.00002 \text{ keV}^{-1} .$$

The fact that the coefficient  $b$  contributes at most a few percent correction over a 1 MeV range confirms the suitability of our expression for the calibration. The statistical uncertainty is not given for this calibration curve since the other uncertainties such as setting of the discrimination level and the nature of the calibration formula are more important. A conservative estimate of the present calibration uncertainty is  $\pm 5\%$  near the 1 MeV region and  $\pm 7\%$  near the 300 keV region.

In addition to the basic test of parity change, linear polarization measurements can also be used to remove ambiguities in spin assignment which exist if only angular distribution information is available. For example, the same values for  $A_{22}$  and  $A_{44}$  can be obtained for a quadrupole transition between states with  $\Delta I = 2$  and a highly mixed transition between states with  $\Delta I = 0$ . Nevertheless the value of  $P$  will be quite different since  $H_k = 1$  for the pure quadrupole and  $H_k \neq 1$  for the mixed transition. For example, when  $A_{22} = +0.31$  and  $A_{44} = -0.099$  (typical values for a

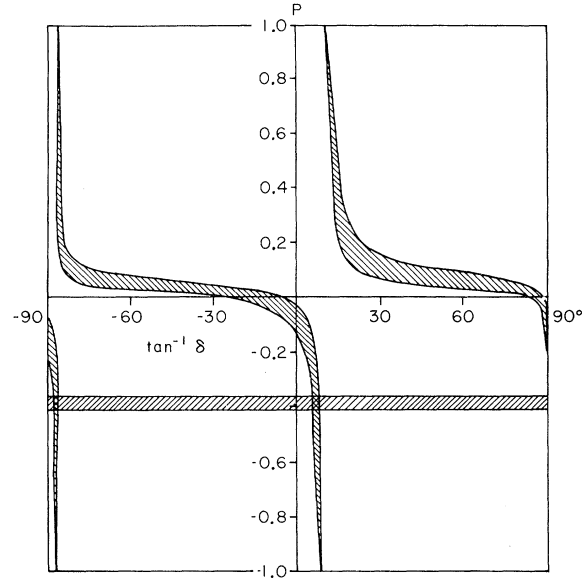


FIG. 3. Analysis of the polarization data for the determination of the  $M1$ - $E2$  mixing ratio for the 264-keV transition in  $^{99}\text{Pd}$ . The region of overlap corresponding to an almost pure  $E2$  is discarded as unrealistic on the ground of angular distribution.

quadrupole transition),  $P \approx +0.5$  for  $\Delta I = 2$  and  $P \approx -0.1$  for  $\Delta I = 0$  ( $\delta \approx 1.5$ ).

The procedure for analyzing an  $M1$ - $E2$  mixing ratio is illustrated in Fig. 3 where the allowed region based on angular distribution data is

TABLE I. Linear polarization data of  $\gamma$  rays following the reaction  $^{92}\text{Zr}(^{12}\text{C}, 3n)^{101}\text{Pd}$ .

$E_\gamma$	$I_i \rightarrow I_f$	$A_{22}$	$A_{44}$	$\Delta$ (measured)	$\Delta$ (calculated)	Multipolarity
261	$\frac{7}{2} \rightarrow \frac{5}{2}$	-0.217 (8)	0.013(10)	-0.16(1)	-0.15(1)	$M1$
406	$\frac{9}{2} \rightarrow \frac{7}{2}$	-0.145(19)	0.060(50)	-0.06(5)	-0.09(1)	$M1$
556	$\frac{15}{2} \rightarrow \frac{11}{2}$	0.322(10)	-0.114(13)	0.19(1)	0.19(2)	$E2$
657	$\frac{21}{2} \rightarrow \frac{17}{2}$	0.343(11)	-0.121(13)	0.19(2)	0.19(2)	$E2$
667	$\frac{9}{2} \rightarrow \frac{5}{2}$	0.309(10)	-0.091(11)	0.18(1)	0.17(1)	$E2$
670	$\frac{11}{2} \rightarrow \frac{9}{2}$	-0.228(10)	0.008 (9)	0.10(1)	0.13(1)	$E1$
678	$\frac{11}{2} \rightarrow \frac{7}{2}$	0.309(10)	-0.091(10)	0.17(2)	0.17(1)	$E2$
736	$\frac{13}{2} \rightarrow \frac{9}{2}$	0.319 (9)	-0.099(11)	0.16(3)	0.17(1)	$E2$
748	$\frac{19}{2} \rightarrow \frac{15}{2}$	0.346(10)	-0.126(13)	0.14(2)	0.18(1)	$E2$
804	$\frac{17}{2} \rightarrow \frac{13}{2}$	0.331(10)	-0.102(11)	0.20(2)	0.17(1)	$E2$
878	$\frac{15}{2} \rightarrow \frac{11}{2}$	0.304(13)	-0.091(41)	0.13(2)	0.14(1)	$E2$
891	$\frac{23}{2} \rightarrow \frac{19}{2}$	0.312(16)	-0.145(25)	0.17(3)	0.14(1)	$E2$
904	$\frac{19}{2} \rightarrow \frac{15}{2}$	0.278(13)	-0.109(17)	0.12(3)	0.12(1)	$E2$
947	$\frac{25}{2} \rightarrow \frac{21}{2}$	0.295(14)	-0.054(27)	0.10(3)	0.13(1)	$E2$

TABLE II. Linear polarization data of  $\gamma$  rays following the reaction  $^{94}\text{Zr}(^{12}\text{C}, 3n)^{103}\text{Pd}$ .

$E_\gamma$	$I_i \rightarrow I_f$	$A_{22}$	$A_{44}$	$\Delta$ (measured)	$\Delta$ (calculated)	Multipolarity	$\delta$
186	$\frac{9}{2} \rightarrow \frac{7}{2}$	-0.241 (9)	0.027(10)	-0.00(6)	-0.17(1)	<i>M1</i> <i>M1-E2</i>	... -4.7 < $\delta$ < -0.16
237	$\frac{15}{2} \rightarrow \frac{17}{2}$	-0.170(12)	0.043(10)	-0.06(5)	-0.12(1)	<i>M1</i> <i>M1-E2</i>	... -0.03 < $\delta$ < 0.36
	$\frac{19}{2} \rightarrow \frac{17}{2}$				-0.16(3)	<i>M1-E2</i>	0.01 < $\delta$ < 0.05 <sup>a</sup>
244	$\frac{7}{2} \rightarrow \frac{5}{2}$	-0.271 (8)	0.019 (6)	-0.10(1)	-0.18(1)	<i>M1</i> <i>M1-E2</i>	... -0.10 < $\delta$ < -0.07
256	$\frac{21}{2} \rightarrow \frac{19}{2}$	-0.272(26)	0.012(35)	-0.12(9)	-0.18(2)	<i>M1</i> <i>M1-E2</i>	... -0.25 < $\delta$ < 0.01
311	$\frac{17}{2} \rightarrow \frac{15}{2}$	-0.094(20)	0.004(29)	-0.29(6)	-0.06(2)	<i>M1</i> <i>M1-E2</i>	... 0.07 < $\delta$ < 0.13
332	$\frac{17}{2} \rightarrow \frac{15}{2}$	-0.154(20)	0.019(26)	-0.20(5)	-0.10(2)	<i>M1</i> <i>M1-E2</i>	... 0.04 < $\delta$ < 0.07
446	$\frac{19}{2} \rightarrow \frac{17}{2}$	-0.075(43)	0.027(71)	-0.18(8)	-0.04(3)	<i>M1</i> <i>M1-E2</i>	... 0.02 < $\delta$ < 0.12
451	$\frac{9}{2} \rightarrow \frac{5}{2}$	0.240(23)	-0.115(32)	0.23(9)	0.14(2)	<i>E2</i>	...
474	$\frac{9}{2} \rightarrow \frac{7}{2}$	-0.452(26)	0.078(32)	0.07(3)	-0.23(2)	<i>M1</i> <i>M1-E2</i>	... -6.3 < $\delta$ < -0.8
477	$\frac{15}{2} \rightarrow \frac{11}{2}$	0.318 (8)	-0.107 (9)	0.24(1)	0.21(2)	<i>E2</i>	...
532	$\frac{7}{2} \rightarrow \frac{5}{2}$	-0.557(18)	0.054(12)	0.03(2)	-0.25(2)	<i>M1</i> <i>M1-E2</i>	... -0.9 < $\delta$ < -0.5
541	$\frac{11}{2} \rightarrow \frac{7}{2}$	0.165(30)	-0.090(34)	-0.10(6)	-0.08(2)	<i>M2</i>	...
660	$\frac{11}{2} \rightarrow \frac{7}{2}$	0.289 (9)	-0.097(10)	0.22(2)	0.16(2)	<i>E2</i>	...
714	$\frac{19}{2} \rightarrow \frac{15}{2}$	0.307 (8)	-0.114(10)	0.17(1)	0.16(1)	<i>E2</i>	...
718	$\frac{9}{2} \rightarrow \frac{5}{2}$	0.201 (9)	-0.056(10)	0.12(2)	0.10(1)	<i>E2</i>	...
809	$\frac{13}{2} \rightarrow \frac{9}{2}$	0.237(19)	-0.076(21)	0.23(6)	0.12(4)	<i>E2</i>	...
847	$\frac{23}{2} \rightarrow \frac{19}{2}$	0.273(19)	-0.106(21)	0.18(2)	0.15(3)	<i>E2</i>	...
873	$\frac{15}{2} \rightarrow \frac{11}{2}$	0.298(17)	-0.084(20)	0.14(2)	0.14(2)	<i>E2</i>	...
970	$\frac{27}{2} \rightarrow \frac{23}{2}$	0.346(50)	-0.106(40)	0.12(2)	0.15(3)	<i>E2</i>	...
987	$\frac{19}{2} \rightarrow \frac{15}{2}$	0.309(19)	-0.153(31)	0.17(5)	0.12(2)	<i>E2</i>	...

<sup>a</sup>  $\delta$  limited by angular distribution data. See text.

depicted in a diagram of polarization versus the tangent of the mixing ratio for the 264-keV transition in  $^{99}\text{Pd}$ . The polarization data from the present experiment are also shown as a horizontal zone. The overlapping regions represent the possible assignment of mixing ratio. In the present case the region corresponding to an almost pure *E2* ( $\delta \rightarrow -\infty$ ) is excluded as unrealistic on the basis of angular distribution data, and the value  $0.10 < \delta < 0.14$  is adopted. Notice in this example that much poorer statistics in the polarization determination would not have affected the mixing ratio determination appreciably. This last feature persisted in most of the mixed transitions in  $^{99}\text{Pd}$ .

#### IV. RESULTS

The results are presented for each isotope in Tables I, II, and III. In each table, the first column designates the transition energy; the second column lists the spin assignments for the initial and final states as obtained from the previous angular distribution experiments<sup>8,9</sup> and the present linear polarization measurements; the third and fourth column give the angular distribution coefficients; the fifth column shows the experimental asymmetry  $\Delta$ ; and the sixth column lists the asymmetry obtained from the angular distribution coefficients with the assumption that

TABLE III. Linear polarization data of  $\gamma$  rays following the reaction  $^{90}\text{Zr}(^{12}\text{C}, 3n)^{90}\text{Pd}$ .

$E_\gamma$	$I_i \rightarrow I_f$	$A_{22}$	$A_{44}$	$\Delta$ (measured)	$\Delta$ (calculated)	Multipolarity	$\delta$
264	$\frac{7}{2} \rightarrow \frac{5}{2}$	-0.075(25)	0.033(29)	-0.19(1)	-0.05(2)	$M1$ $M1-E2$	...
338	$\frac{17}{2} \rightarrow \frac{15}{2}$	-0.270(25)	0.046(28)	-0.17(2)	-0.16(2)	$M1$	$0.10 < \delta < 0.14$ ...
398	$\frac{13}{2} \rightarrow \frac{15}{2}$	-0.118(16)	0.030(16)	-0.19(1)	-0.07(1)	$M1$ $M1-E2$	...
493	$\frac{15}{2} \rightarrow \frac{13}{2}$	-0.215(15)	0.007(16)	-0.16(1)	-0.12(1)	$M1$ $M1-E2$	...
531	$\frac{21}{2} \rightarrow \frac{19}{2}$	-0.287(30)	0.068(40)	-0.11(4)	-0.15(2)	$M1$	$0.02 < \delta < 0.05$ ...
649	$\frac{15}{2} \rightarrow \frac{11}{2}$	0.365(16)	-0.145(23)	0.15(1)	0.20(2)	$E2$	...
778	$\frac{9}{2} \rightarrow \frac{5}{2}$	0.342 (9)	-0.105(12)	0.17(1)	0.18(1)	$E2$	...
805	$\frac{11}{2} \rightarrow \frac{7}{2}$	0.318(10)	-0.100(13)	0.15(1)	0.16(1)	$E2$	...
860	$\frac{13}{2} \rightarrow \frac{9}{2}$	0.316(16)	-0.111(19)	0.16(1)	0.15(1)	$E2$	...
881	$\frac{19}{2} \rightarrow \frac{15}{2}$	0.289(16)	-0.079(18)	0.11(2)	0.13(1)	$E2$	...
891	$\frac{17}{2} \rightarrow \frac{13}{2}$	0.307(15)	-0.097(20)	0.15(2)	0.14(1)	$E2$	...
911	$\frac{23}{2} \rightarrow \frac{19}{2}$	0.313(20)	-0.124(26)	0.10(3)	0.14(2)	$E2$	...
955	$\frac{19}{2} \rightarrow \frac{15}{2}$	0.329(28)	-0.109(30)	0.21(4)	0.15(2)	$E2$	...
1114	$\frac{23}{2} \rightarrow \frac{19}{2}$	0.317(49)	-0.092(51)		0.13(3)	$E2$	...
1117		-0.243(33)	0.035(46)		-0.083(10) +0.083(10)	$M1$ $E1$	...
1114-1117				0.094(21)	+0.100(12) <sup>a</sup>		...

<sup>a</sup> Intensity weighted average of the 1114-keV  $\gamma$  ray and 1117-keV ( $E1$ )  $\gamma$  ray. These  $\gamma$  rays were clearly resolved in the angular distribution experiment but not in the linear polarization measurement.

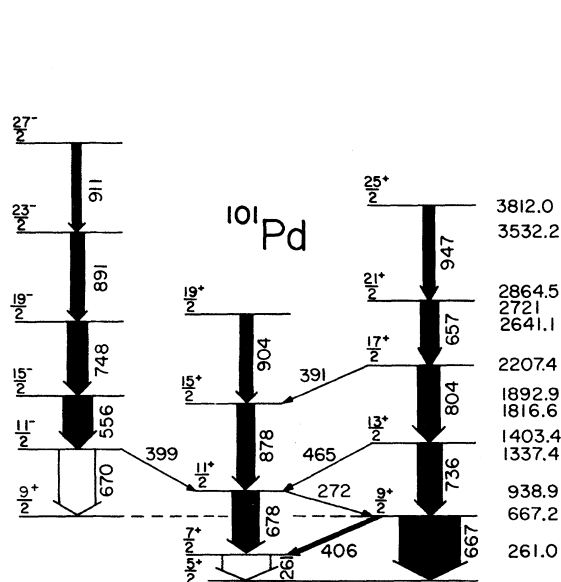


FIG. 4. Decay scheme of  $^{101}\text{Pd}$  following the reaction  $^{92}\text{Zr}(^{12}\text{C}, 3n)$ .  $E2$  transitions are shown as darkened arrows.

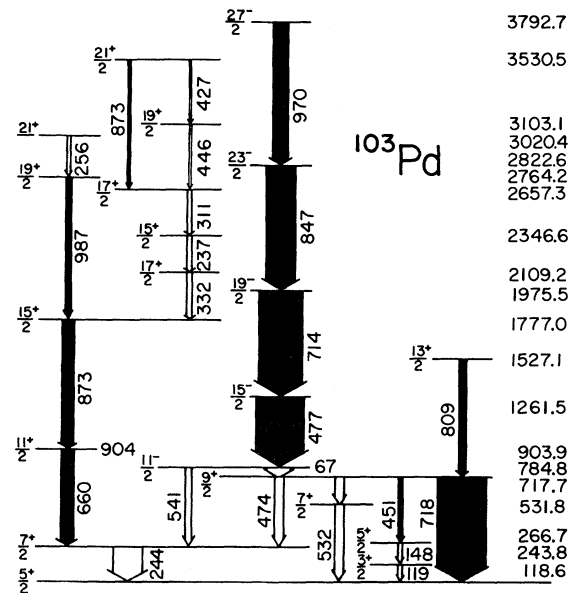


FIG. 5. Decay scheme of  $^{103}\text{Pd}$  following the reaction  $^{94}\text{Zr}(^{12}\text{C}, 3n)$ .  $E2$  transitions are shown as darkened arrows.

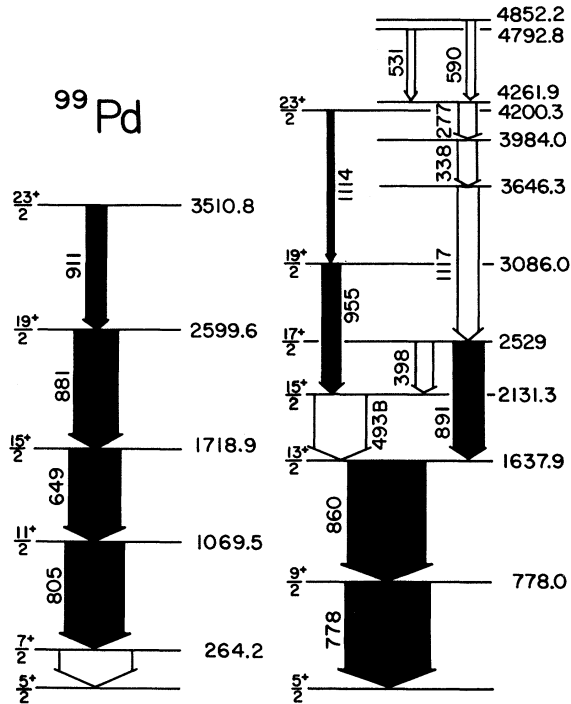


FIG. 6. Decay scheme of  $^{99}\text{Pd}$  following the reaction  $^{90}\text{Zr}(^{12}\text{C}, 3n)$ .  $E2$  transitions are shown as darkened arrows.

the transition is a pure multipole. When the calculated value of  $\Delta$  for a pure transition was not in agreement with the observed  $\Delta$ , the mixing ratio  $\delta$  was adjusted to bring the calculated and observed values of  $\Delta$  into agreement. These results for  $\delta$  are given in the last column. Partial decay schemes for the three isotopes which show the transitions of interest are presented in Figs. 4-6.

The most important result of the linear polarization measurements for  $^{101}\text{Pd}$  (Table I) is that the 670-keV  $\gamma$  ray is definitely  $E1$ . Thus the 1337.38-keV state shown in Fig. 4 is the expected  $\frac{11}{2}^-$  state. In addition, all transitions in the three bands are confirmed as being  $E2$  multipoles (shown as dark arrows in Fig. 4). The possibility of some of these transitions connecting states with  $\Delta I = 0$  is eliminated. It is interesting that the 261-keV transition from the  $\frac{7}{2}^+$  bandhead to the ground state is very pure in  $^{101}\text{Pd}$  while the corresponding transitions in  $^{99}\text{Pd}$  and  $^{103}\text{Pd}$  have significant  $E2$  contributions.

The results for  $^{103}\text{Pd}$  are given in Table II. The linear polarization indicates that the 541-keV  $\gamma$  ray comes from an  $M2$  transition which changes parity. Thus, the 784.8-keV state most likely has spin and parity  $\frac{11}{2}^-$ . However, in this case the linear polarization does not give a unique

answer because it is also possible that the 541-keV  $\gamma$  ray is emitted in a highly mixed  $\frac{7}{2}^+ - \frac{7}{2}^+$  transition. Since there is considerable other evidence<sup>9</sup> for the  $\frac{11}{2}^-$  assignment it is considered certain. All of the transitions shown in Fig. 5 as dark arrows are confirmed as being electric quadrupoles.

The 237-keV transition is a good example of another case where the linear polarization gives information about the spin sequence which is not provided by the angular distribution alone. The angular distribution coefficients are consistent with either a  $\frac{15}{2}^+ - \frac{17}{2}^+$  or  $\frac{19}{2}^+ - \frac{17}{2}^+$  sequence. General trends would suggest that the higher spin value ( $\frac{19}{2}^+$ ) is correct. However when the mixing ratio that is consistent with the angular distribution data is used to calculate  $\Delta$  for a  $\frac{19}{2}^+ - \frac{17}{2}^+$  transition, the result is not consistent with  $\Delta$  (measured) as shown in Table II. On the other hand the angular distribution and linear polarization are both in agreement with a  $\frac{15}{2}^+ - \frac{17}{2}^+$  assignment.

For some transitions, the angular distribution measurement gives better limits for the mixing ratios. (For example, the 186-keV transition has  $-0.18 \leq \delta \leq -0.06$  from the angular distribution<sup>9</sup> and  $-4.7 \leq \delta \leq 0.16$  from the linear polarization.) However in other cases the results from the linear polarization are better. (For the 244-keV transition,  $-0.1 \leq \delta \leq -0.07$  from linear polarization and  $-0.15 \leq \delta \leq -0.05$  from the angular distribution.<sup>9</sup>) For  $^{103}\text{Pd}$  it is interesting to note that all of the  $\Delta I = 1$  transitions have substantial  $E2$  mixtures.

A partial decay scheme for  $^{99}\text{Pd}$  which was developed from  $(\text{HI}, xn)$  experiments<sup>10</sup> is shown in Fig. 6. The  $\frac{7}{2}^+$  band in  $^{99}\text{Pd}$  is very similar to the corresponding bands in  $^{101}, ^{103}\text{Pd}$ , but the other transitions in  $^{99}\text{Pd}$  show very little similarity to  $^{101}, ^{103}\text{Pd}$ . Targets are not available to study  $^{99}\text{Pd}$  with light particle transfer reactions, and radioactive decay experiments are so difficult that they have not been performed. In the absence of these experiments and systematic trends, standard  $(\text{HI}, xn)$  measurements are not adequate to determine the spin and parity of many important states.

Fortunately the linear polarization experiments are a great aid in establishing the decay scheme. All transitions identified with dark arrows in Fig. 6 are shown to be  $E2$  in Table III. Thus the angular momentum values given are almost certainly unique. (It is possible that the angular momentum of states in an  $E2$  cascade go down by two units at any step rather than up, but this is highly unlikely.)

The 1117-keV transition is very important because the results at the bottom of Table III indi-

cate that this is an  $E1$  transition. The analysis is complicated by the fact that the 1114- and 1117-keV transitions were not resolved in the linear polarization detector. Fortunately these  $\gamma$  rays were clearly resolved in the angular distribution experiment, so that values of  $\Delta$  can be calculated reliably and an intensity weighted average can be obtained. The results in the table which are in good agreement with  $\Delta(\text{measured})$  assume that the 1117-keV transition is  $E1$ . If it is  $M1$ , the intensity weighted average would be  $-0.005(12)$ .

Another complication is the fact that the three transition 277, 338, and 1117 keV have essentially the same intensity, so it is difficult to determine their sequence. There are some weak transitions which support the order shown in Fig. 6, but this ordering must at best be considered tentative. If the order is correct, then the states at 3646.3, 3984.0, 4261.9, 4792.8, and 4852.2 keV must all have *negative* parity. If the 1117-keV  $\gamma$  ray precedes the 277- and 338-keV  $\gamma$  rays, then only the three highest energy states would have negative parity. In either case, these high spin negative parity states are most unusual. The states do *not* appear to be part of a band built on the  $\frac{11}{2}^-$  state. Although the spin of the state that emits the 1117-

keV  $\gamma$  ray has not yet been definitely established, it is most likely at least  $\frac{13}{2}^-$ . The  $\frac{15}{2}^-$  and  $\frac{17}{2}^-$  states apparently are not observed. The transitions which do connect the negative parity states are dipoles not quadrupoles, and finally the two states near 4800 keV do not fit into a band interpretation.

It is not surprising that the  $\frac{11}{2}^-$  band was not observed in  $^{99}\text{Pd}$ . The systematic trend for the  $\frac{11}{2}^-$  state in the nuclei  $^{105}, ^{103}, ^{101}\text{Pd}$  suggests that this state would be located at approximately 2000 keV in  $^{99}\text{Pd}$ . With this high bandhead energy, the members of the  $\frac{11}{2}^-$  band are not expected to be yrast states.

Since  $^{99}\text{Pd}$  has four proton holes and three neutron particles outside the closed 50 shell, the unusual negative parity states may be the result of a three quasiparticle configuration. For example  $(1h_{11/2})^1 (2d_{5/2})^2$  or  $(1h_{11/2})^1 (1g_{7/2})^2$  configurations could have the observed spin and parity. Additional experiments are being performed to improve the decay scheme of  $^{99}\text{Pd}$ . This is an important nucleus which shows a significant change from the collective effects that are observed in  $^{101}, ^{103}, ^{105}\text{Pd}$ .  $^{99}\text{Pd}$  provides an unusual opportunity to observe the effect of adding a few neutrons above the closed 50 shell.

†Work supported in part by the National Science Foundation and the U. S. Atomic Energy Commission.

\*Present address: Physics Division, Oak Ridge National Laboratory, Oak Ridge, Tennessee 37830.

<sup>1</sup>F. A. Rickey and P. C. Simms, *Phys. Rev. Lett.* **31**, 404 (1973).

<sup>2</sup>F. E. Bertrand, *Nucl. Data B11*, 449 (1974).

<sup>3</sup>P. Taras, *Can. J. Phys.* **49**, 328 (1971).

<sup>4</sup>K. Hardy, A. Lumpkin, Y. K. Lee, and G. E. Owen, *Rev. Sci. Instrum.* **42**, 482 (1971).

<sup>5</sup>A. H. Lumpkin, A. W. Sunyar, K. A. Hardy, and Y. K.

Lee, *Phys. Rev. C* **9**, 258 (1974).

<sup>6</sup>T. Yamazaki, *Nucl. Data A3*, 1 (1967).

<sup>7</sup>K. S. Krane and R. M. Steffen, *Phys. Rev. C* **2**, 724 (1970).

<sup>8</sup>P. C. Simms, G. J. Smith, F. A. Rickey, J. A. Grau, J. R. Tesmer, and R. M. Steffen, *Phys. Rev. C* **9**, 684 (1974).

<sup>9</sup>J. A. Grau, F. A. Rickey, G. J. Smith, P. C. Simms, and J. R. Tesmer, *Nucl. Phys. A229*, 346 (1974).

<sup>10</sup>G. J. Smith, J. A. Grau, F. A. Rickey, P. C. Simms, and J. R. Tesmer (unpublished).